


## Reversible linear-compression behavior of free volume in a metallic glass

Songyi Chen,<sup>1</sup> Dazhe Xu,<sup>1</sup> Xin Zhang,<sup>1</sup> Xiehang Chen,<sup>1</sup> Ye Liu,<sup>1</sup> Tao Liang,<sup>1,2</sup> Ziliang Yin,<sup>1</sup> Sheng Jiang,<sup>3</sup> Ke Yang,<sup>3</sup> Jianrong Zeng,<sup>3</sup> Hongbo Lou,<sup>1</sup> Zhidan Zeng,<sup>1</sup> and Qiaoshi Zeng<sup>1,\*</sup>

<sup>1</sup>Center for High Pressure Science and Technology Advanced Research, Pudong, Shanghai 201203, People's Republic of China

<sup>2</sup>Jiangsu Key Laboratory of Advanced Metallic Materials, School of Materials Science and Engineering, Southeast University, Nanjing 211189, People's Republic of China

<sup>3</sup>Shanghai Synchrotron Radiation Facility, Shanghai Advanced Research Institute, Chinese Academy of Sciences, Shanghai 201210, People's Republic of China

 (Received 9 February 2022; revised 17 March 2022; accepted 22 March 2022; published 4 April 2022)

Free volume is one of the key structural concepts widely used to describe various glass phenomena. However, free volume is challenging to be rigorously defined in glass structures and directly determined by experiments. Here, we employed metallic glass as a simple glass model system and studied the structural evolution of an as-spun (hyperquenched) and another thermally annealed metallic glass with different amounts of free volume by *in situ* high-pressure synchrotron x-ray diffraction. Therefore, the effect of free volume on the compression behavior of metallic glasses can be clarified by comparing the two samples at identical experimental conditions. We find that a higher amount of free volume causes both lower density and bulk modulus as expected at ambient conditions. Surprisingly, during compression, the decrease of free volume has a constant rate up to  $\sim 30$  GPa and appears to be mostly reversible upon decompression without obvious permanent densification after pressure release. These results suggest an elastic process in metallic glasses under pressure. Implications of these results for the structural models based on the free-volume concept are discussed. The typically assumed glass structural model with isolated domains of “liquidlike” (free-volume rich) region embedded in a solidlike (free-volume poor) matrix seems unlikely. Instead, a more “homogeneous” model over a wide range of length scales such as a nested fractal network of liquid- and solidlike regions seems more consistent with the experimental observation.

DOI: [10.1103/PhysRevB.105.144201](https://doi.org/10.1103/PhysRevB.105.144201)

Glass usually forms via fast quenching of its melt, in which the melt falls out of equilibrium and its disordered structure is frozen by bypassing crystallization. Considerable excess atomic volume, so-called free volume, is frozen and inherited in glass from melt [1,2]. Free volume has been one of the most important concepts widely used to describe and quantify complex glass phenomena and properties, such as viscosity [2], glass transition [3–5], relaxation [6,7], diffusion [1,8], deformation [9–12], etc. Although the free-volume concept is intuitively understandable as the space for a molecule to move freely inside a cage forming by the molecule/atom's nearest neighbors, it is structurally ill defined given complex disordered glass or liquid structures [13]. Moreover, direct and accurate determination of free volume is challenging to conventional experimental diagnostic probes. Nevertheless, efforts to derive more fundamental descriptions and constraints on free volume from experiments are desirable and critical to deepening our understanding of the glassy structure and behavior [14].

Metallic glasses (MGs) [15] are believed to have random close packing of atoms with nondirectional metallic bonds, and therefore regarded as one of the simplest glass systems, which could benefit the fundamental studies of glasses in

general [3]. Based on the free-volume concept, the total volume of a MG basically consists of quench-in free volume,  $V_{\text{free}}$ , and the limiting, fixed, hard-core volume of atoms,  $V_{\text{hc}}$ . Furthermore, free volume,  $V_{\text{free}}$ , is considered to be made up of two parts, i.e., the temperature-dependent extra atomic volume due to thermal vibration,  $V_{\text{free:vib}}$ , and the temperature-independent excess free volume due to the specific disordered glassy configuration,  $V_{\text{free:exs}}$  [14].  $V_{\text{free:exs}}$  can be annihilated by thermal annealing below the glass transition temperature,  $T_g$ , and then restored by heating above  $T_g$  or thermal-cycling induced rejuvenation, which usually involves diffusion or so-called nonaffine displacement of atoms and significantly affects the properties of MGs [16,17].  $V_{\text{free:vib}}$  is a sort of “occupied volume” also existing in the crystalline solid state, and therefore independent of glass thermal history. Glasses that only differ in the amounts of  $V_{\text{free:exs}}$  due to different thermal history show identical thermal expansion coefficient since the thermal expansion in glasses is mainly controlled by  $V_{\text{free:vib}}$  [7]. Similarly, the compression behavior would also be expected to be controlled by the backbones/elastic matrix consisting of  $V_{\text{free:vib}}$  and  $V_{\text{hc}}$ , and therefore independent of thermal history ( $V_{\text{free:exs}}$  values) [18]. This can be explained by the theory that far below the glass transition temperatures, the structural rearrangement is kinetically arrested in glasses; therefore, response to changes in temperature and pressure is usually believed not to involve structural rearrangement, leading to constant free volumes [19]. However, as-prepared and

\*zengqs@hpstar.ac.cn

annealed MGs have been extensively reported to have quite different bulk moduli [20]. Moreover, permanent densification was reported in MGs after high-pressure treatment even at room temperature, which is attributed to the pressure-induced annihilation of free volume, although lacking direct evidence [21,22]. Therefore, many open questions remain regarding the pressure effect on the free volume in MGs, e.g., how does the free volume annihilate under high pressure at room temperature? Is there a critical pressure required for the free-volume annihilation and permanent densification, and to what extent could the free volume be annihilated? By addressing these questions, we could even derive long-sought fundamental information about how free volume spatially distributes in MGs. To achieve that, we need to accurately monitor the free volume in MGs during compression and decompression. Recently, synchrotron x-ray diffraction (XRD) has been demonstrated to be an effective and accurate *in situ* probe to characterize the variation of free volume in MGs [7]. Therefore, in this work, we employ *in situ* high-pressure synchrotron XRD to monitor the free volume as a function of pressure up to 30 GPa in MGs with different initial free-volume levels (i.e., as-spun and thermally annealed MGs). The compression behavior of the two MGs can be directly associated with their free-volume contents. By revealing the role of free volume upon compression and decompression, our results provide critical validation of the existing models and theories of the free volume in MGs and may promote our understanding of various glass phenomena.

$\text{Cu}_{46}\text{Zr}_{46}\text{Al}_8$ , as an extensively studied prototype ternary bulk MG system, has good glass-forming ability and a wide supercooled liquid region [23].  $\text{Cu}_{46}\text{Zr}_{46}\text{Al}_8$  MGs were reported to have good plasticity as well [24,25], which usually suggests a high amount of free volume in this system. Therefore, it is chosen as a model system for this work. Master alloy ingots of  $\sim 30$  g with the nominal composition of  $\text{Cu}_{46}\text{Zr}_{46}\text{Al}_8$  were prepared by arc melting of pure elements with a purity ranging from 99.9 to (99.99 at. %) under an argon atmosphere. Each ingot was remelted five times to ensure a chemically homogeneous master alloy. Ribbon samples with thicknesses of approximately  $20 \mu\text{m}$  were obtained by melt spinning with a copper wheel speed of 50 m/s.

Thermal analyses were performed using a differential scanning calorimeter (PerkinElmer DSC-8500) under continuous high-purity nitrogen (99.999 at. %) gas flow. A typical heating rate of 20 K/min was applied. Thermal annealing of the MG ribbons was performed in the DSC furnace under a flowing high-purity nitrogen atmosphere. The annealing temperature was set to be 648 K (the glass transition temperature,  $T_g$ , is  $\sim 723$  K) and then maintained for 3600 s before being cooled down quickly to room temperature, which will be referred to as the annealed MG sample in the following text.

The structural characterization of the samples using XRD and small-angle x-ray scattering (SAXS) at ambient conditions was carried out at the beamlines 15U1 and 16B1, respectively, at Shanghai synchrotron radiation facility (SSRF), China. The wavelength of the monochromatic x-ray beam was  $0.6199 \text{ \AA}$  at the beamline 15U1 and  $1.0332 \text{ \AA}$  at the beamline 16B1. The exposure time of each pattern was 30 s for XRD and 60 s for SAXS.

For *in situ* high-pressure synchrotron XRD experiments, the as-spun and annealed MG ribbon samples were cut into small pieces with different shapes (rectangle and triangle, respectively) and then loaded together into one symmetric diamond-anvil cell (DAC) [26] with a diamond culet size of  $\sim 400 \mu\text{m}$ . The sample chamber is a hole of  $\sim 120 \mu\text{m}$  drilled by laser in a preindented T301 stainless steel. Helium was loaded as the pressure-transmitting medium to provide the best hydrostatic pressure condition up to tens of GPa [27]. Small ruby balls and a piece of gold foil were also loaded in the sample chamber near the MG samples using the ruby fluorescence peak or Au equation of state to calibrate the pressure inside the sample chamber. Pressure was controlled by a double-side membrane system [28]. The pressure was stabilized with a fluctuation of less than 0.2 GPa before and after each XRD exposure. The *in situ* high-pressure XRD experiments were carried out at the beamline 15U1 at SSRF, China. A monochromatic x-ray beam was focused down to approximately  $2.5 \times 3 \mu\text{m}^2$  by a Kirkpatrick-Baez mirror system. Two-dimensional (2D) diffraction images were collected with a Mar165 charge-coupled device detector. The exposure time for each pressure point was 20 s. The background scattering from the high-pressure environment was also taken next to the sample where the x-ray beam only went through the pressure medium helium and two diamonds anvils.

The as-spun and annealed MG samples were characterized by synchrotron XRD and SAXS as shown in Figs. 1(a) and 1(b), respectively, which confirm their homogeneous and fully amorphous structures without any detectable crystallization or phase separation. A slight shift of the primary diffraction peak position by  $\sim 0.6\%$  (from  $2.694$  to  $2.710 \text{ \AA}^{-1}$ ) and peak width narrowing by  $\sim 6.4\%$  (full width at half maximum from  $0.492$  to  $0.460 \text{ \AA}^{-1}$ ) is detected after annealing, which suggests densification and ordering of the glass structure as expected. The hyperquenched as-spun ribbon MGs usually preserve a high amount of quench-in free volume, which is confirmed in the as-spun  $\text{Cu}_{46}\text{Zr}_{46}\text{Al}_8$  MG by a large exothermic signal (starts at  $\sim 450$  K) below  $T_g$  due to structural relaxation as shown in Fig. 2(a) [29,30]. To get samples with different amounts of free volume for a comparison study, isothermal annealing below  $T_g$  is the most extensively employed method [31]. Therefore, the as-spun samples were annealed at 648 K ( $0.9 T_g$ ) for different duration time. The enthalpy difference upon annealing [ $\Delta H$ , Fig. 2(a)] is directly associated with the annihilation of free volume in the samples towards more stable states, which follows a stretched exponential Kohlrausch-Williams-Watts function with a relaxation time of  $\sim 623$  s [Fig. 2(b)]. To have low amount of free volume but avoid possible crystallization, eventually the sample with annealing time of 3600 s was chosen as the comparison sample.

After obtaining two  $\text{Cu}_{46}\text{Zr}_{46}\text{Al}_8$  MG samples with distinct amounts of free volume, we are able to use *in situ* high-pressure XRD to address how the different amounts of free volume in MGs could affect their compression behavior. Since the difference between the two samples in structure/density revealed by XRD is still quite small (peak shift by  $\sim 0.5\%$ ), reliable measurements require simultaneous determination of the variation of structure and pressure for both samples with identical experimental resolution and accuracy. To achieve

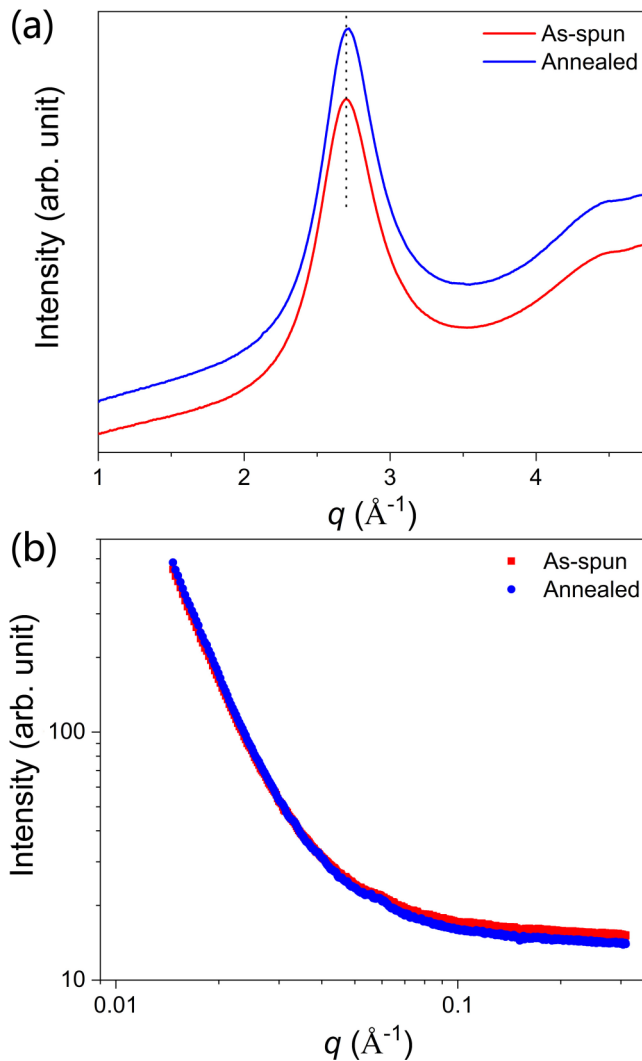


FIG. 1. Structural characterization of the as-spun and annealed  $\text{Cu}_{46}\text{Zr}_{46}\text{Al}_8$  MG samples. (a) Synchrotron XRD patterns. No sharp Bragg diffraction peaks due to crystallization is detected. The vertical dashed line marks the principal peak position of the as-spun sample. (b) SAXS patterns. The smoothly decayed intensity without bumps rules out any nanoscale density fluctuation due to crystallization or phase separation. The tiny kinks at  $\sim 0.6 \text{ \AA}^{-1}$  in the SAXS patterns for both samples are from the detector.

that, we loaded an as-spun and an annealed MG samples into one DAC at the same time and used helium as the pressure-transmitting medium [as shown in the inset of Fig. 3(a)] and started XRD pattern collection only when each pressure was stabilized. Figure 3 shows *in situ* high-pressure XRD patterns during compression for the as-spun and annealed  $\text{Cu}_{46}\text{Zr}_{46}\text{Al}_8$  MG alloys. It is clear that the principal XRD peaks of both samples shift to higher  $q$  values with increasing pressure due to pressure-induced shrinkage of atomic spacing. The almost constant XRD peak width of both samples indicates no noticeable structural changes in terms of structural order variation. The XRD patterns with a high signal-to-noise ratio allow us to determine their peak positions accurately. The principal peak positions,  $q_1$ , as a function of pressure [Fig. 4(a)] were derived by fitting with a Voigt line profile. Interestingly, the

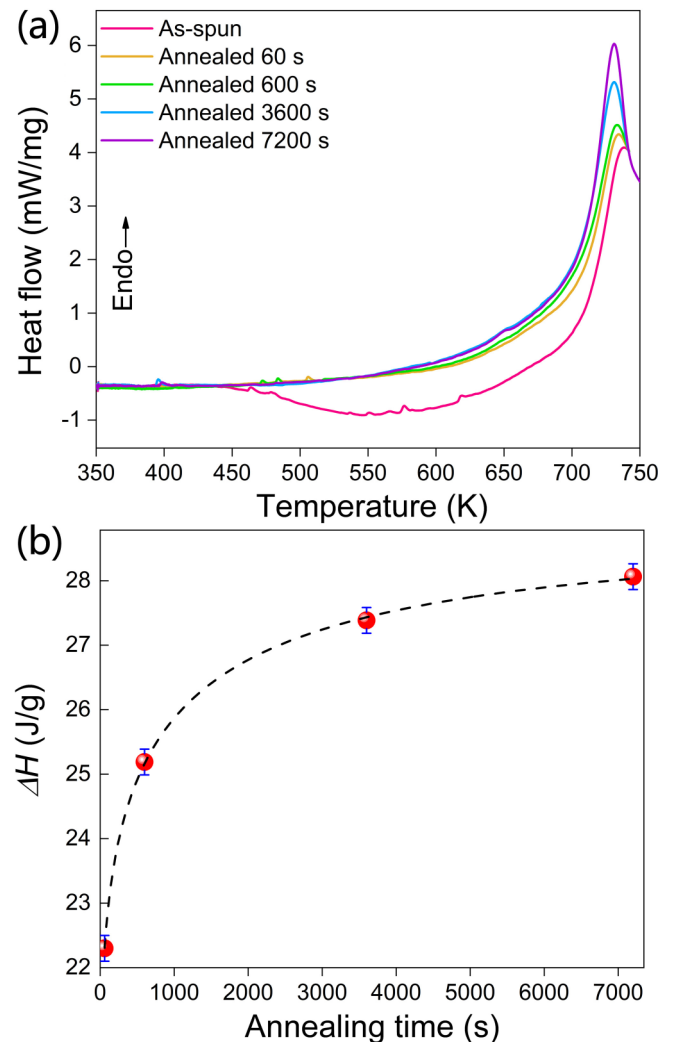


FIG. 2. DSC characterization of the as-spun and annealed  $\text{Cu}_{46}\text{Zr}_{46}\text{Al}_8$  MG samples with different annealing time. (a) DSC traces of the as-spun sample and samples annealed at 648 K ( $0.9 T_g$ ) for 60, 600, 3600, and 7200 s. (b) Enthalpy difference in the DSC traces shown in (a) as a function of annealing time between the annealed and the as-spun samples.

$q_1$  values of the two samples get very close to each other at high pressures, although they are pretty different at ambient and relatively low pressures. But during decompression, although not many data points are available, the recovered difference between the  $q_1$  values of the two samples below 5 GPa indicates that the compression behavior is mostly reversible, and no obvious permanent structural change is observed in either sample. It should be noted the *in situ* high-pressure synchrotron XRD technique employed in this work is an atomic structure probe, which could avoid influence of the collapse of common casting micro- and nanopores on the estimation of atomic packing density change during compression.

The annealed MG sample with less free volume is intuitively expected to be more incompressible than the as-spun MG sample, which is consistent with our experimental observation of the always larger  $q_{1\text{-annealed}}$  than  $q_{1\text{-as-spun}}$  in Fig. 4(a).

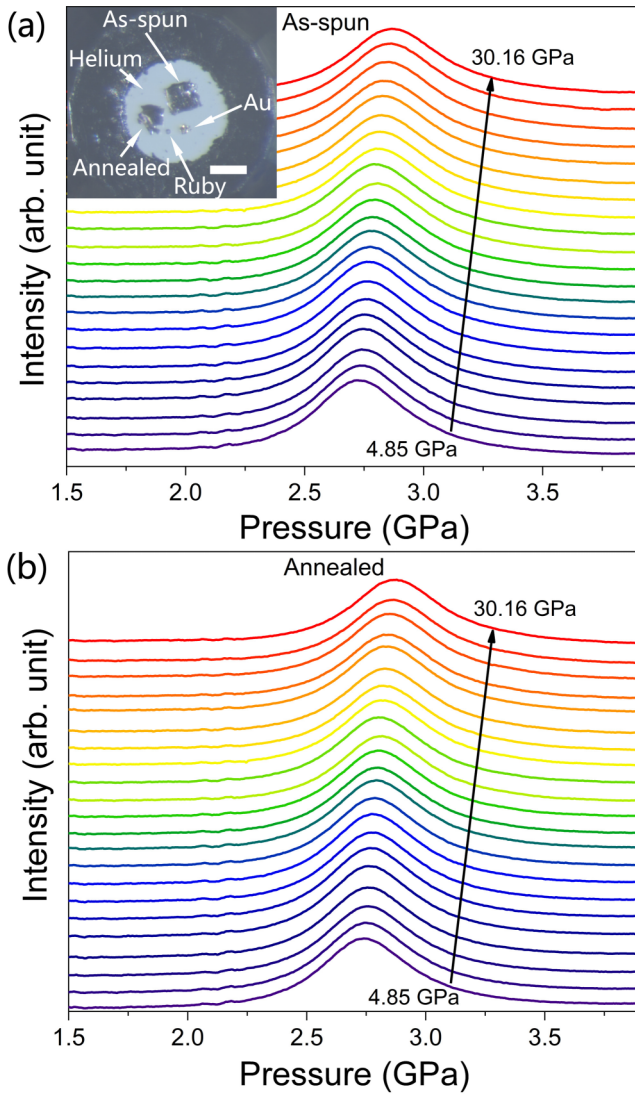


FIG. 3. *In situ* high-pressure XRD patterns of  $\text{Cu}_{46}\text{Zr}_{46}\text{Al}_8$  MGs during compression at room temperature. (a) As-spun sample. (b) Annealed sample. The inset in (a) is the image of two samples loaded together in one DAC with helium as the pressure medium. The scale bar represents  $70 \mu\text{m}$ .

The inverse XRD peak position  $q_1$  is believed to correlate with the average atomic volume  $V_a$  in MGs by a simple power-law relationship, i.e.,  $V_a \propto (1/q_1)^D$  [32], which thus could reflect the structural evolution with volume variance under pressure [33,34]. The exponent  $D$  of the power law varies in a narrow range below 3 depending on the specific composition. For the Zr-based MGs,  $D$  was experimentally determined to be  $\sim 2.6$  [33,34]. Therefore, the sample volume as a function of pressure can be estimated by  $V_a \propto (1/q_1)^{2.6}$  for the  $\text{Cu}_{46}\text{Zr}_{46}\text{Al}_8$  MG. The diverged pressure dependence of normalized volume change  $V/V_0$  in Fig. 4(b) confirms our expectation that the as-spun MG sample is more compressible than the annealed sample. The data of volume versus pressure can be fitted by the third-order Birch-Murnaghan isothermal equation of state (BM-EOS) [35]. The fit yields the isothermal bulk modulus ( $B_0$ ) and the pressure derivative ( $B'$ ). For the as-spun sample,  $B_0 = 129 \pm 2 \text{ GPa}$  and  $B' = 4.2 \pm 0.2$ , while for the

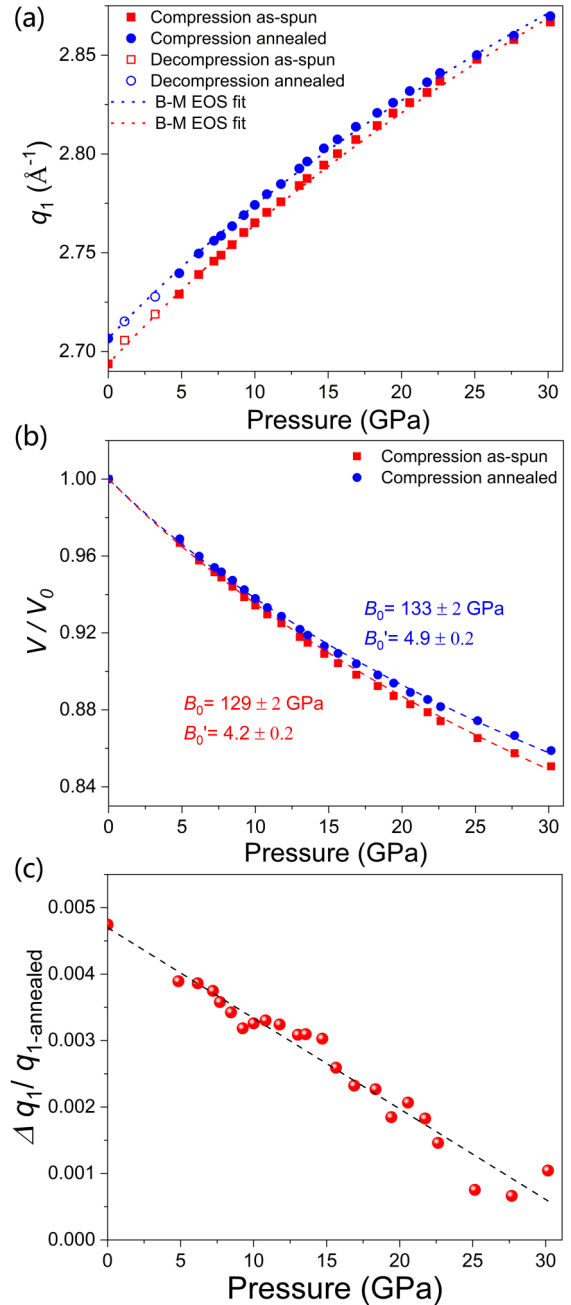


FIG. 4. Analysis of the principal diffraction peak position change as a function of pressure. (a)  $q_1$  values of the as-spun and annealed samples as a function of pressure. The relatively big pressure step from 0 GPa to  $\sim 5$  GPa was due to overtightening of the membrane system during assemblage. Two sets of data from decompression are plotted together for comparison, as shown in open symbols. The dashed lines are the fits to the third-order BM-EOS derived from (b). The major errors are from the pressure differences determined before and after each XRD exposure and the fitting uncertainty of each XRD peak position. Error bars are smaller than the symbol sizes. (b) Relative volume change as a function of pressure estimated by the power law of  $q_1$ ,  $(q_{1,0\text{GPa}}/q_{1,P})^{2.6} = V(P)/V(0 \text{ GPa})$ . The dashed lines are the fits to the third-order BM-EOS, which yields the isothermal bulk modulus ( $B_0$ ) and the pressure derivative ( $B'$ ). (c) Relative difference change of  $q_1$  between the as-spun and annealed samples,  $\Delta q_1/q_{1\text{-annealed}} = q_{1\text{-as-spun}} - q_{1\text{-annealed}}/q_{1\text{-annealed}}$  as a function of pressure. The dashed line is a linear fit of the data.



annealed sample,  $B_0 = 133 \pm 2$  GPa and  $B' = 4.9 \pm 0.2$ , which are quite consistent with previous reported bulk moduli measured by ultrasonic technique [24]. Therefore, the data in Fig. 4(a) can be interpreted that the as-spun sample with smaller bulk modulus decreases its overall volume faster than the annealed sample and seemingly approaches the annealed sample state with increasing pressure. With this point in mind, the approaching rate of the as-spun state to the annealed state can be estimated by the pressure dependence of the relative difference in  $q_1$ , i.e.,  $q_{1\text{-as-spun}} - q_{1\text{-annealed}}/q_{1\text{-annealed}}$ , as shown in Fig. 4(c). Surprisingly, the  $\Delta q_1/q_{1\text{-annealed}}$  shows a linearly decreasing trend with increasing pressure up to 30 GPa.

These results suggest that the free volume does affect the compression behavior of MGs, but the detailed information is not in line with our expectations based on previous models or results. Specifically, for the linear pressure dependence of  $\Delta q_1/q_{1\text{-annealed}}$ , it means the compression of MGs is not solely controlled by the occupied volume ( $V_{\text{free:vib}} + V_{\text{hc}}$ ); otherwise, the as-spun and annealed  $\text{Cu}_{46}\text{Zr}_{46}\text{Al}_8$  MG should show identical compressibility similar to the thermal expansion experiments reported before. In the thermal expansion experiments of MGs, the amount of free volume is believed to be frozen and keeps as a constant at temperatures far below  $T_g$  [19]. Therefore, MGs with different energy states (also differ in specific volume) but the identical composition will always show parallel thermal expansion volume curves. According to our experiment result, it seems that the free volume is compressible. And, the higher amount of free volume an MG has, the more compressible the MG will be. Moreover, the linear relationship between  $\Delta q_1/q_{1\text{-annealed}}$  and pressure over the entire pressure range indicates that no critical pressure is required to squeeze out free volume in MGs. A simple model will be the free volume is somehow homogeneously mixed with the matrix consisting of occupied volume from microscopic to macroscopic scales. Again, otherwise, for a quite inhomogeneous model typically proposed as the liquidlike (with more free volume) regions (domains) that exist as inclusions in the solidlike matrix, it is expected to have inhomogeneous compression curves, i.e., at the low-pressure region, the hydrostatic pressure will be mainly sustained by the matrix framework. Then, as the pressure increases beyond the yield point of the matrix, the liquidlike inclusion will suddenly contribute the most compressibility. In this case, the sample with more free volume will appear suddenly more compressible above a certain threshold pressure. However, this is not observed in this work; instead, the compression curves of both samples are smooth, which can be perfectly fitted by a single BM-EOS. The excess free volume in the as-spun sample linearly decreases to approach the annealed sample. Therefore, a glass structure with spatially well-mixed solid- and liquidlike regions are proposed based on our experiment, which could most likely be a percolation network without isolated domains and support the percolation theory for glass forming through a glass transition [3]. The recent studies trying to map the distribution of properties in MGs do extensively find spatial fluctuation, mostly with a fractal distribution rather than isolated domains [36,37], which is in line with our scenario.

Permanent annihilation of free volume under high pressure appears unlikely in the  $\text{Cu}_{46}\text{Zr}_{46}\text{Al}_8$  MG at room temperature regarding the mostly reversible compression behavior. On the other hand, it suggests that the decrease of free volume during compression is most likely associated with pressure-induced nonaffine elastic deformation due to the diverse responses of each component to pressure in multicomponent MGs. Therefore, the pressure-suppressed free volume in MGs could be different from the diffusion-mediated free-volume annihilation during thermal annealing. During decompression, the  $q_1$  values of both samples almost follow the initial compression curve without noticeable hysteresis by the generation of more free volume in the compression and decompression cycle. These phenomena also demonstrate that the glass structure in MGs is quite robust, and overall it basically remains in the elastic deformation regime during compression; therefore, a heterogeneous model with a distinct solidlike matrix plus a liquidlike inclusion could not survive and reproduce the results observed in this work.

In contrast, it has been reported that many amorphous materials have permanent densification after high-pressure treatment. For instance, the amorphous  $\text{SiO}_2$  may have  $\sim 21\%$  density increase after compressing to 25 GPa at room temperature [21], which is believed to be associated with a significant decrease of the intertetrahedral angle (Si-O-Si angles), slight or undetectable changes of the interatomic distances, and a gradual increase of the average atomic coordination (from 4 to 6). This scenario can be easily understandable in the open network systems such as  $a\text{-B}_2\text{O}_3$ ,  $a\text{-GeSe}_4$ ,  $a\text{-GeO}_2$ , *et al.*, while in the closely packed structures of MGs with already very high coordination numbers, e.g., even up to 12–14 random nearest neighbors, there is not much open space to collapse during compression. In some previous studies on MGs with high-pressure treatment at high temperatures, permanent densification was reported [38–41], which could be caused by local rearrangement of atomic structures via thermally activated diffusion. Instead, during compression at room temperature, most of the free volume can be compressed but cannot be permanently annihilated, suggesting a quite homogeneously distribution of free volume in a stiff network. It should be noted that since our experiments were carried out at room temperature rather than absolute 0 K, slight structural relaxation/diffusion might still occur during the experiments under high pressure, which may contribute to the minute deviation ( $\Delta q_1$ ) of the decompression data from the fitting curve of the compression data as shown in Fig. 4(a) ( $\Delta q_1 = 0.026\%$  at 3.2 GPa and  $\Delta q_1 = 0.12\%$  at 1.1 GPa during decompression for the as-prepared  $\text{Cu}_{46}\text{Zr}_{46}\text{Al}_8$  MG, and  $\Delta q_1 = -0.095\%$  at 3.2 GPa and  $\Delta q_1 = 0.0015\%$  at 1.1 GPa for the annealed  $\text{Cu}_{46}\text{Zr}_{46}\text{Al}_8$  MGs.).

In summary, *in situ* high-pressure synchrotron XRD measurement was carried out on the as-spun and annealed  $\text{Cu}_{46}\text{Zr}_{46}\text{Al}_8$  MGs with identical experimental conditions by loading them together into the same DAC. High-quality XRD data were obtained during compression up to  $\sim 30$  GPa and decompression back to ambient pressure with carefully stabilized pressures. These data enable us to reliably resolve

the slight difference in the XRD peak positions between two samples due to their different amounts of free volume. The as-spun sample with higher free-volume content than the annealed sample was found to be more compressible over the entire pressure range studied. The extra free volume in the as-spun sample compared with the annealed sample decreases with a constant rate during compression. In addition, the compression behavior of both samples is mostly reversible during decompression, and no apparent permanent densification was observed in either sample. These results are not in line with the expectation of the simplified heterogeneous structural model for MGs, in which liquidlike regions with more free volume exist as isolated domains in a solidlike matrix with less free volume. Instead, the results in this work consistently suggest well-mixed liquid- and solidlike regions over a considerable length scale, most likely a nested fractal percola-

tion network. These findings provide experimental constraints on the structural model of free volume in MGs, which could help to further complete the free-volume theory and deepen our understanding of MGs in terms of atomic structure and structure-dictated properties.

This work was supported by the National Natural Science Foundation of China (Grants No. 51871054 and No. U1930401). The XRD and SAXS experiments were performed at the beamlines 15U1 and 16B1 of Shanghai Synchrotron Radiation Facility (SSRF), respectively. The authors thank Dr. Haiyun Shu for his kind help with the gas loading system, Dr. Cheng Wen Mao for the beamline support at 15U1, SSRF, and Dr. Jingshi Wu from Stanford University, USA for her help with the experiments and the helpful discussion.

- 
- [1] M. H. Cohen and D. Turnbull, Molecular transport in liquids and glasses, *J. Chem. Phys.* **31**, 1164 (1959).
- [2] A. K. Doolittle, Studies in Newtonian flow. II. The dependence of the viscosity of liquids on free-space, *J. Appl. Phys.* **22**, 1471 (1951).
- [3] M. H. Cohen and G. S. Grest, Liquid-glass transition, a free-volume approach, *Phys. Rev. B* **20**, 1077 (1979).
- [4] D. Turnbull and M. H. Cohen, Free-volume model of the amorphous phase: Glass transition, *J. Chem. Phys.* **34**, 120 (1961).
- [5] P. Wen, M. B. Tang, M. X. Pan, D. Q. Zhao, Z. Zhang, and W. H. Wang, Calorimetric glass transition in bulk metallic glass forming Zr-Ti-Cu-Ni-Be alloys as a free-volume-related kinetic phenomenon, *Phys. Rev. B* **67**, 212201 (2003).
- [6] O. Haruyama and A. Inoue, Free volume kinetics during sub-T<sub>g</sub> structural relaxation of a bulk Pd<sub>40</sub>Ni<sub>40</sub>P<sub>20</sub> metallic glass, *Appl. Phys. Lett.* **88**, 131906 (2006).
- [7] A. R. Yavari, A. L. Moulec, A. Inoue, N. Nishiyama, N. Lupu, E. Matsubara, W. J. Botta, G. Vaughan, M. D. Michiel, and Å. Kvick, Excess free volume in metallic glasses measured by X-ray diffraction, *Acta Mater.* **53**, 1611 (2005).
- [8] K. Rätzke, P. W. Hüppe, and F. Faupel, Transition from Single-Jump Type to Highly Cooperative Diffusion during Structural Relaxation of a Metallic Glass, *Phys. Rev. Lett.* **68**, 2347 (1992).
- [9] P. S. Steif, F. Spaepen, and J. W. Hutchinson, Strain localization in amorphous metals, *Acta Metall.* **30**, 447 (1982).
- [10] A. S. Argon and H. Y. Kuo, Plastic flow in a disordered bubble raft (an analog of a metallic glass), *Mater. Sci. Eng.* **39**, 101 (1979).
- [11] W. Dmowski, T. Iwashita, C. P. Chuang, J. Almer, and T. Egami, Elastic Heterogeneity in Metallic Glasses, *Phys. Rev. Lett.* **105**, 205502 (2010).
- [12] J. C. Ye, J. Lu, C. T. Liu, Q. Wang, and Y. Yang, Atomistic free-volume zones and inelastic deformation of metallic glasses, *Nat. Mater.* **9**, 619 (2010).
- [13] T. G. Fox and P. J. Flory, The glass temperature and related properties of polystyrene. Influence of molecular weight, *J. Polym. Sci.* **14**, 315 (1954).
- [14] R. P. White and J. E. G. Lipson, Polymer free volume and its connection to the glass transition, *Macromolecules* **49**, 3987 (2016).
- [15] H. W. Sheng, W. K. Luo, F. M. Alamgir, J. M. Bai, and E. Ma, Atomic packing and short-to-medium-range order in metallic glasses, *Nature (London)* **439**, 419 (2006).
- [16] S. V. Ketov, Y. H. Sun, S. Nachum, Z. Lu, A. Checchi, A. R. Beraldin, H. Y. Bai, W. H. Wang, D. V. Louzguine-Luzgin, M. A. Carpenter *et al.*, Rejuvenation of metallic glasses by non-affine thermal strain, *Nature (London)* **524**, 200 (2015).
- [17] C. Nagel, K. Rätzke, E. Schmidtke, J. Wolff, U. Geyer, and F. Faupel, Free-volume changes in the bulk metallic glass Zr<sub>46.7</sub>Ti<sub>8.3</sub>Cu<sub>7.5</sub>Ni<sub>10</sub>Be<sub>27.5</sub> and the undercooled liquid, *Phys. Rev. B* **57**, 10224 (1998).
- [18] A. J. Matheson, Role of free volume in the pressure dependence of the viscosity of liquids, *J. Chem. Phys.* **44**, 695 (1966).
- [19] C. T. Moynihan, P. B. Macedo, C. J. Montrose, C. J. Montrose, P. K. Gupta, M. A. DeBolt, J. F. Dill, B. E. Dom, P. W. Drake, A. J. Eastale *et al.*, Structural relaxation in vitreous materials, *Ann. N. Y. Acad. Sci.* **279**, 15 (1976).
- [20] W. H. Wang, The elastic properties, elastic models and elastic perspectives of metallic glasses, *Prog. Mater. Sci.* **57**, 487 (2012).
- [21] T. Rouxel, H. Ji, T. Hammouda, and A. Moréac, Poisson's Ratio and the Densification of Glass under High Pressure, *Phys. Rev. Lett.* **100**, 225501 (2008).
- [22] T. P. Ge, C. Wang, J. Tan, T. Ma, X. H. Yu, C. Q. Jin, W. H. Wang, and H. Y. Bai, Unusual energy state evolution in Ce-based metallic glass under high pressure, *J. Appl. Phys.* **121**, 205109 (2017).
- [23] W. H. Wang, J. J. Lewandowski, and A. L. Greer, Understanding the glass-forming Ability of Cu<sub>50</sub>Zr<sub>50</sub> alloys in terms of a metastable eutectic, *J. Mater. Res.* **20**, 2307 (2011).
- [24] Q. K. Jiang, X. D. Wang, X. P. Nie, G. Q. Zhang, H. Ma, H. J. Fecht, J. Bendnarcik, H. Franz, Y. G. Liu, Q. P. Cao *et al.*, Zr-(Cu,Ag)-Al bulk metallic glasses, *Acta Mater.* **56**, 1785 (2008).
- [25] C. Liu, E. Pineda, and D. Crespo, Characterization of mechanical relaxation in a Cu-Zr-Al metallic glass, *J. Alloys Compd.* **643**, S17 (2015).

- [26] H.-K. Mao, B. Chen, J. Chen, K. Li, J.-F. Lin, W. Yang, and H. Zheng, Recent advances in high-pressure science and technology, *Matter Radiat. Extrem.* **1**, 59 (2016).
- [27] S. Klotz, J. C. Chervin, P. Munsch, and G. Le Marchand, Hydrostatic limits of 11 pressure transmitting media, *J. Phys. D* **42**, 075413 (2009).
- [28] W. B. Daniels and M. G. Ryschkewitsch, Simple double diaphragm press for diamond anvil cells at low temperatures, *Rev. Sci. Instrum.* **54**, 115 (1983).
- [29] A. van den Beukel and J. Sietsma, The glass transition as a free volume related kinetic phenomenon, *Acta Metall. Mater.* **38**, 383 (1990).
- [30] L. Hu, C. Zhou, C. Zhang, and Y. Yue, Thermodynamic anomaly of the sub-T<sub>g</sub> relaxation in hyperquenched metallic glasses, *J. Chem. Phys.* **138**, 174508 (2013).
- [31] M. E. Launey, J. J. Kruzic, C. Li, and R. Busch, Quantification of free volume differences in a Zr<sub>44</sub>Ti<sub>11</sub>Ni<sub>10</sub>Cu<sub>10</sub>Be<sub>25</sub> bulk amorphous alloy, *Appl. Phys. Lett.* **91**, 051913 (2007).
- [32] D. Ma, A. D. Stoica, and X. L. Wang, Power-law scaling and fractal nature of medium-range order in metallic glasses, *Nat. Mater.* **8**, 30 (2009).
- [33] Q. Zeng, Y. Kono, Y. Lin, Z. Zeng, J. Wang, S. V. Sinogeikin, C. Park, Y. Meng, W. Yang, and H.-K. Mao, Universal Fractional Noncubic Power Law for Density of Metallic Glasses, *Phys. Rev. Lett.* **112**, 185502 (2014).
- [34] Q. Zeng, Y. Lin, Y. Liu, Z. Zeng, C. Y. Shi, B. Zhang, H. Lou, S. V. Sinogeikin, Y. Kono, and C. Kenney-Benson, General 2.5 power law of metallic glasses, *Proc. Natl. Acad. Sci.* **113**, 1714 (2016).
- [35] F. Birch, Elasticity and constitution of the Earth interior, *J. Geophys. Res.* **57**, 227 (1952).
- [36] Y. Yang, J. F. Zeng, A. Volland, J. J. Blandin, S. Gravier, and C. T. Liu, Fractal growth of the dense-packing phase in annealed metallic glass imaged by high-resolution atomic force microscopy, *Acta Mater.* **60**, 5260 (2012).
- [37] B. Huang, T. P. Ge, G. L. Liu, J. H. Luan, Q. F. He, Q. X. Yuan, W. X. Huang, K. Zhang, H. Y. Bai, C. H. Shek *et al.*, Density fluctuations with fractal order in metallic glasses detected by synchrotron X-ray nano-computed tomography, *Acta Mater.* **155**, 69 (2018).
- [38] R. J. Xue, L. Z. Zhao, C. L. Shi, T. Ma, X. K. Xi, M. Gao, P. W. Zhu, P. Wen, X. H. Yu, C. Q. Jin *et al.*, Enhanced kinetic stability of a bulk metallic glass by high pressure, *Appl. Phys. Lett.* **109**, 221904 (2016).
- [39] R. Yamada, Y. Shibasaki, Y. Abe, W. Ryu, and J. Saida, Unveiling a new type of ultradense anomalous metallic glass with improved strength and ductility through a high-pressure heat treatment, *NPG Asia Mater.* **11**, 72 (2019).
- [40] W. Dmowski, G. H. Yoo, S. Gierlotka, H. Wang, Y. Yokoyama, E. S. Park, S. Stelmakh, and T. Egami, High pressure quenched glasses: Unique structures and properties, *Sci. Rep.* **10**, 9497 (2020).
- [41] H. J. Jin, X. J. Gu, P. Wen, L. B. Wang, and K. Lu, Pressure effect on the structural relaxation and glass transition in metallic glasses, *Acta Mater.* **51**, 6219 (2003).